



## CMS RPC L1 Trigger clustering at CMSSW



C. Giordano <sup>1</sup>, M. Tytgat <sup>2</sup>, K. Mota Amarilo <sup>3</sup>, A. Samalan <sup>3</sup>, K. Skovpen <sup>3</sup>, G.A. Alves <sup>4</sup>, E. Alves Coelho <sup>4</sup>, F. Marujo da Silva <sup>4</sup>, M. Barroso Ferreira Filho <sup>5</sup>, E.M. Da Costa <sup>5</sup>, D. De Jesus Damiao <sup>5</sup>, B.C. Ferreira <sup>5</sup>, S. Fonseca De Souza <sup>5</sup>, L. Mundim <sup>5</sup>, H. Nogima <sup>5</sup>, J.P. Pinheiro <sup>5</sup>, A. Santoro <sup>5</sup>, R. Gomes De Souza <sup>5</sup>, M. Thiel <sup>5</sup>, A. Aleksandrov <sup>6</sup>, R. Hadjiska <sup>6</sup>, P. Iaydjiev <sup>6</sup>, M. Shopova <sup>6</sup>, G. Sultanov <sup>6</sup>, A. Dimitrov <sup>7</sup>, L. Litov <sup>7</sup>, B. Pavlov <sup>7</sup>, P. Petkov <sup>7</sup>, A. Petrov <sup>7</sup>, E. Shumka <sup>7</sup>, P. Cao <sup>8</sup>, W. Diao <sup>8</sup>, W. Gong <sup>8</sup>, Q. Hou <sup>8</sup>, H. Kou <sup>8</sup>, Z.-A. Liu <sup>8</sup>, J. Song <sup>8</sup>, N. Wang <sup>8</sup>, J. Zhao <sup>8</sup>, S.J. Qian <sup>9</sup>, C. Avila <sup>10</sup>, D.A. Barbosa Trujillo <sup>10</sup>, A. Cabrera <sup>10</sup>, C.A. Florez <sup>10</sup>, J.A. Reyes Vega <sup>10</sup>, R. Aly <sup>10,12</sup>, A. Radi <sup>11</sup>, Y. Assran <sup>12</sup>, I. Crotty <sup>13</sup>, M.A. Mahmoud <sup>13</sup>, L. Balleyguier <sup>14</sup>, X. Chen <sup>14</sup>, C. Combaret <sup>14</sup>, G. Galbit <sup>14</sup>, M. Gouzevitch <sup>14</sup>, G. Grenier <sup>14</sup>, I.B. Laktineh <sup>14</sup>, A. Luciol <sup>14</sup>, L. Mirabito <sup>14</sup>, W. Tromeur <sup>14</sup>, I. Bagaturia <sup>15</sup>, O. Kemularia <sup>15</sup>, I. Lomidze <sup>15</sup>, Z. Tsamalaidze <sup>15</sup>, V. Amoozegar <sup>16</sup>, B. Boghrati <sup>16</sup>, M. Ebrahimi <sup>16</sup>, F. Esfandi <sup>16</sup>, Y. Hosseini <sup>16</sup>, M. Mohammadi Najafabadi <sup>16</sup>, E. Zareian <sup>16</sup>, M. Abbrescia <sup>17,18</sup>, N. De Filippis <sup>17,19</sup>, G. Iaselli <sup>17,19</sup>, F. Loddo <sup>17</sup>, G. Pugliese <sup>17,19</sup>, D. Ramos <sup>17</sup>, L. Benussi <sup>20</sup>, S. Bianco <sup>20</sup>, S. Meola <sup>20</sup>, D. Piccolo <sup>20</sup>, S. Buontempo <sup>21</sup>, F. Carnevali <sup>21,22</sup>, L. Lista <sup>21,22</sup>, P. Paolucci <sup>21</sup>, A. Braghieri <sup>24</sup>, P. Montagna <sup>24,25</sup>, C. Riccardi <sup>24,25</sup>, P. Salvini <sup>24</sup>, P. Vitulo <sup>24,25</sup>, F. Fienga <sup>23</sup>, T.J. Kim <sup>26</sup>, E. Asilar <sup>26</sup>, Y. Ryou <sup>26</sup>, S. Choi <sup>27</sup>, B. Hong <sup>27</sup>, K.S. Lee <sup>27</sup>, J. Goh <sup>28</sup>, J. Shin <sup>28</sup>, Y. Lee <sup>29</sup>, I. Pedraza <sup>30</sup>, C. Uribe Estrada <sup>30</sup>, H. Castilla-Valdez <sup>31</sup>, R. Lopez-Fernandez <sup>31</sup>, A. Sánchez Hernández <sup>31</sup>, M. Ramírez García <sup>32</sup>, D.L. Ramirez Guadarrama <sup>32</sup>, M.A. Shah <sup>32</sup>, E. Vazquez <sup>32</sup>, N. Zaganidis <sup>32</sup>, A. Ahmad <sup>33</sup>, M.I. Asghar <sup>33</sup>, H.R. Hoorani <sup>33</sup>, S. Muhammad <sup>33</sup>, J. Eysermans <sup>34</sup>, on behalf of the CMS Collaboration

<sup>1</sup> Department of High Energy Physics at Austrian Academy of Sciences, Vienna, Austria<sup>2</sup> Vrije Universiteit Brussel, Brussel, Belgium<sup>3</sup> Universiteit Gent, Gent, Belgium<sup>4</sup> Centro Brasileiro de Pesquisas Fisicas, Rio de Janeiro, Brazil<sup>5</sup> Universidade do Estado do Rio de Janeiro, Rio de Janeiro, Brazil<sup>6</sup> Institute for Nuclear Research and Nuclear Energy, Bulgarian Academy of Sciences, Sofia, Bulgaria<sup>\*</sup> Corresponding author.E-mail address: [cristina.giordano@cern.ch](mailto:cristina.giordano@cern.ch) (C. Giordano).<sup>a</sup> Also at Technical University, Vienna, Austria.<sup>b</sup> Also at Ghent University, Ghent, Belgium.<sup>c</sup> Now at UERJ, Rio de Janeiro, Brazil.<sup>d</sup> Now at PSI, Villigen, Switzerland.<sup>e</sup> Also at Academy of Scientific Research and Technology of the Arab Republic of Egypt, Egyptian Network of High Energy Physics, Cairo, Egypt.<sup>f</sup> Also at Sultan Qaboos University, Muscat, Oman.<sup>g</sup> Also at Suez University, Suez, Egypt.<sup>h</sup> Also at an institute or an international laboratory covered by a cooperation agreement with CERN.<sup>i</sup> Also at Università degli Studi Guglielmo Marconi, Roma, Italy.<sup>j</sup> Also at Scuola Superiore Meridionale, Università di Napoli 'Federico II', Napoli, Italy.<sup>k</sup> Also at CERN, European Organization for Nuclear Research, Geneva, Switzerland.

<sup>7</sup> Faculty of Physics, University of Sofia, Sofia, Bulgaria  
<sup>8</sup> Institute of High Energy Physics and University of the Chinese Academy of Sciences, Beijing, China  
<sup>9</sup> School of Physics, Peking University, Beijing, China  
<sup>10</sup> Universidad de Los Andes, Bogota, Colombia  
<sup>11</sup> Department of Physics, Faculty of Science, Ain Shams University, Cairo, Egypt  
<sup>12</sup> The British University in Egypt, Cairo, Egypt  
<sup>13</sup> Center for High Energy Physics (CHEP-FU), Fayoum University, El-Fayoum, Egypt  
<sup>14</sup> Institut de Physique des 2 Infinis de Lyon, Villeurbanne, France  
<sup>15</sup> Georgian Technical University, Tbilisi, Georgia  
<sup>16</sup> Institute for Research in Fundamental Sciences, Tehran, Iran  
<sup>17</sup> INFN Sezione di Bari, Bari, Italy  
<sup>18</sup> Università di Bari, Bari, Italy  
<sup>19</sup> Politecnico di Bari, Bari, Italy  
<sup>20</sup> INFN Laboratori Nazionali di Frascati, Frascati, Italy  
<sup>21</sup> INFN Sezione di Napoli, Napoli, Italy  
<sup>22</sup> Università di Napoli 'Federico II', Napoli, Italy  
<sup>23</sup> Dipartimento di Ingegneria Elettrica e delle Tecnologie dell'Informazione - Università Degli Studi di Napoli Federico II, Napoli, Italy  
<sup>24</sup> INFN Sezione di Pavia, Pavia, Italy  
<sup>25</sup> Università di Pavia, Pavia, Italy  
<sup>26</sup> Hanyang University, Seoul, Republic of Korea  
<sup>27</sup> Korea University, Seoul, Republic of Korea  
<sup>28</sup> Kyung Hee University, Department of Physics, Seoul, Republic of Korea  
<sup>29</sup> Sungkyunkwan University, Suwon, Republic of Korea  
<sup>30</sup> Benemerita Universidad Autonoma de Puebla, Puebla, Mexico  
<sup>31</sup> Centro de Investigacion y de Estudios Avanzados del IPN, Mexico City, Mexico  
<sup>32</sup> Universidad Iberoamericana, Mexico City, Mexico  
<sup>33</sup> National Centre for Physics, Quaid-I-Azam University, Islamabad, Pakistan  
<sup>34</sup> Massachusetts Institute of Technology, Cambridge, MA, USA

## ARTICLE INFO

**Keywords:**  
 CMS experiment  
 RPC  
 iRPC  
 L1-Trigger  
 Phase-2

## ABSTRACT

The Compact Muon Solenoid detector at the Large Hadron Collider is a multipurpose experiment designed for studying proton-proton and heavy-ion collisions. It features a 3.8 T Solenoid magnet, a Silicon tracker, Electromagnetic and Hadronic Calorimeters, and the Muon system. For the High Luminosity LHC, CMS will undergo Phase-2 upgrades to handle higher collision rates, with PileUp increasing from 50 to 140/200 interactions per bunch crossing, collision energy reaching 14 TeV, and peak luminosity rising to  $5 - 7.5 \times 10^{34} \text{ cm}^{-2} \text{s}^{-1}$ . These upgrades aim to enable even more precise Standard Model measurements, improvements in the Higgs sector, and searches for Beyond Standard Model physics. This document describes the main features of the Endcap Muon Track Finder ++ algorithm, developed in the CMS Software; it is the Level 1 Trigger algorithm upgrade being developed for Phase-2 of the currently used Endcap Track Finder. The efficiency of the algorithm was computed on simulations generated with and without RPC and iRPC ((i)RPC) information, using a pre-trained model.

## 1. The CMS Phase-2 Muon system upgrade

During the Phase-2 upgrade [1], the CMS experiment Muon system will be equipped with new detectors, as well as undergo upgrades of the electronics in order to sustain the new characteristics of the collider machine, brought on by HL-LHC [1]. In the Endcaps of the CMS experiment, there are three subsystems: the Cathode Strip Chambers (CSC), which will be equipped with better electronics, the Gas Electron Multipliers (GEM), which will have an upgraded electronic system and the addition of new chambers in one of the forward stations of the detector MEO, and Resistive Plate Chambers (RPCs), for which both the Link system upgrade and the addition of new improved detectors are expected. The reason behind these planned changes is that the two endcap regions face high muon and background rates and experience less magnetic bending, therefore making it more difficult to reliably trigger on muons in the very forward areas during HL-LHC. To increase the Muon system's redundancy and enable robust track reconstruction — including early rejection of misidentified tracks at the Level-1 (L1) Trigger — the number of hits recorded per track must be increased. The Phase-2 upgrade of the Muon detector aims to restore an effective Muon system in the forward region by introducing new detectors, GE1/1, GE2/1, RE3/1, and RE4/1, which cover the pseudorapidity ( $\eta$ ) range up to 2.4, as shown in Fig. 1. The RPC Link system upgrade aims at improving the time resolution for the existing RPCs, placed in the  $|\eta| < 1.9$  region of the CMS detector; all the off-chamber electronics

will be replaced. Furthermore, in order to sustain the high particle rate and high PileUp (PU) environment of HL-LHC, new improved detectors, called iRPC, will be added to the 2 outer Stations of the CMS Endcap in the  $1.8 < |\eta| < 2.4$  region. They will have an intrinsic time resolution of 0.5 ns.

## 2. The L1 Muon Trigger Phase-2 upgrade

The Phase-2 upgrade of the CMS L1 Trigger system [2] aims to maintain the signal selection efficiency at the level of the Phase-1 system, and also significantly enhance the ability to detect new physics phenomena, including unconventional signatures [2]. The upgraded L1 Trigger will retain a two-level strategy, but the maximum rate will increase to 750 kHz, and the latency will be extended to 12.5  $\mu\text{s}$  to incorporate more detailed detector information, including that coming from the Tracker and the Calorimeter. This extended latency will also support more sophisticated object reconstruction and the evaluation of global event quantities. The system can now consider using particle-flow techniques and machine learning in the trigger algorithms. Additionally, a new 40 MHz scouting system is proposed, which will use trigger primitives (TPs) and objects for real-time analysis, similar to the High-Level Trigger (HLT) scouting system already in place. This scouting system allows for data reduction by storing only high-level information from selected events, enabling searches for event correlations and signatures not easily identified by standard triggers. The Phase-2 L1 Trigger system is designed to handle inputs from various sub-detectors, as shown in Fig. 2. As for the muon trigger,

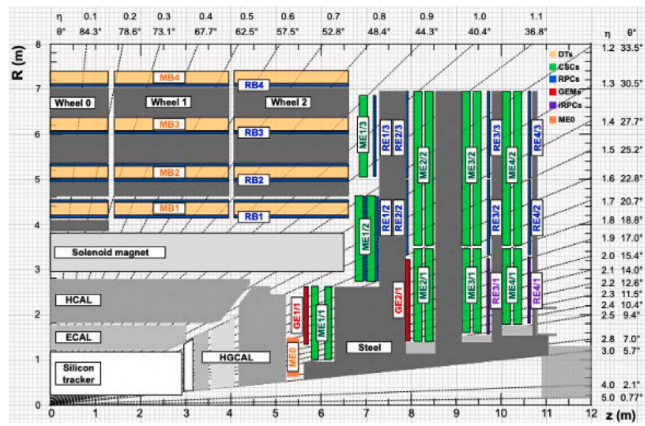


Fig. 1. Cross-section of a quadrant of CMS depicting the Phase-2 upgrades happening in the muon stations RE3/1, RE4/1, GE1/1, GE2/1, and MEO. The locations of the various muon stations are shown in different colours for both the Barrel and the Endcap.

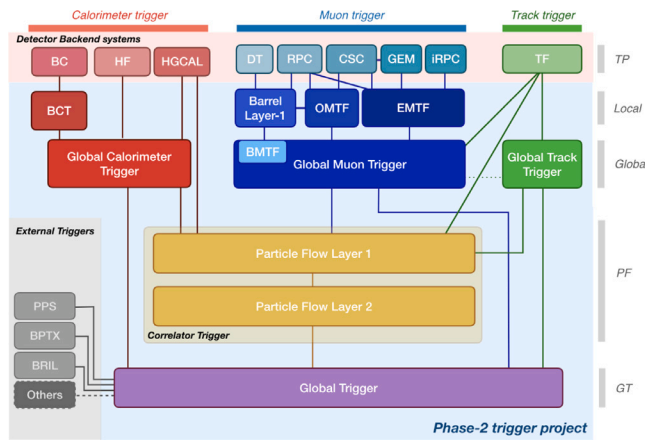


Fig. 2. Functional diagram of the Phase-2 L1 trigger.

after receiving inputs from the various muon detectors, it processes data across different regions through three muon track finders: the Barrel Muon Track Finder (BMTF), the Overlap Muon Track Finder (OMTF) and the Endcap Muon Track Finder (EMTF). Muon candidates and stubs (short tracks, created by high energetic particles when they pass through the tracker) are sent to the Global Muon Trigger (GMT) by EMTF and OMTF, while the BMTF Layer-1, situated inside the GMT, only sends out stubs. The GMT is tasked with sorting the candidates in terms of momentum and quality, removing duplicates and generating track-matched muons and L1 tracks matched to muon stubs.

## 2.1. EMTF++ description

The EMTF++ is the upgrade of the Phase-1 EMTF, which also operates in the  $1.2 < |\eta| < 2.4$  region. It follows the same functionalities of EMTF with a few architectural and structural differences. The first function of the EMTF++ is the TP conversion, in which TPs are converted into EMTF segments, by mapping strips and wires/pads into integer  $\phi$  and  $\eta$  units. After the conversion is complete, EMTF++ can be divided into three main blocks: pattern recognition, track building, and parameter assignment. The algorithm takes as input GEM and iRPC TPs in addition to CSC and RPC ones. The reconstruction algorithm looks for pre-defined patterns, identifying the correlated CSC TPs across multiple stations. These are then matched to RPC TPs, and once the patterns are identified, the track building takes care of attaching segments to the previously identified best tracks. These segments are converted finally

into a set of features that are fed to a Deep Neural Network (DNN) for parameter assignment. The DNN is a feedforward Neural Network with 3 hidden layers that uses information like angular variables and bending information in order to assign momentum and displacement values. While Phase-1 EMTF used a boosted decision tree for this step, the upgraded algorithm uses deep learning in order to enhance the selection efficiency. The EMTF++ algorithm has been developed in the context of the CMS Software (CMSSW), used for many CMS computing activities ranging from data acquisition to data analysis.

## 3. Role of RPC and iRPC

In order to perform efficiency studies enhancing the roles of RPC and iRPC in EMTF++, two separate sets of single muon samples were generated with and without the information coming from RPC/iRPC. The removal of the RPC information allows to see the worsening of the efficiency due to the lack of matching between their TPs and the ones coming from the CSC system. The single muon samples with and without iRPC/RPC inputs were generated with no PU and with an average PU value of 200 with slightly different kinematics characteristics. The PU=200 sample was centrally produced with a flat  $p_T$  distribution between 0 and 200 GeV and a generated  $|\eta|$  range between 1.4 and 3.1. The sample with no PU was privately produced using a custom-made Particle Gun with a flat  $p_T$  distribution between 2 and 120 GeV and a generated  $|\eta|$  range between 1.2 and 2.4. Both samples cover the entire  $-\pi < \phi < \pi$  range. The efficiency is defined by requiring a value of  $\Delta R < 0.1$  between the generated muons and the tracks, where  $\Delta R = \sqrt{(\Delta\eta)^2 + (\Delta\phi)^2}$  indicates the angular distance in the  $\eta - \phi$  plane,  $\phi$  being the azimuthal angle. A  $p_T$  cut is applied on the L1 muons (generated muons) for the numerator (denominator) across all the generated pseudorapidity bins extracted to station 2. Furthermore, a hit quality criterion optimized for single muon samples is applied, requiring at least one hit in station 1 and two hits coming from other stations. Fig. 3 shows the comparison of the efficiencies of EMTF and EMTF++, while Fig. 4 shows the efficiency of the algorithm on the single muon sample generated with the full detector information and no PU for different L1 muon  $p_T$  cuts, showing the stability of the algorithm for higher thresholds. The dips in efficiency around the values of  $|\eta| = 1.2$  and  $|\eta| = 2.4$  are expected because of the fact that the muons triggered at the borders are assigned with a lower quality which leads to a lower efficiency. The additional drops around  $|\eta| = 1.4$  and  $|\eta| = 1.6$  are due to detector geometry constraints. The behaviour for low  $p_T$  cuts in the last two bins is also due to the structure of the detector and resolution effects [2]. Fig. 5 shows the efficiency in bins of generated  $\eta$ , extrapolated to station 2. The plots show the different values of the EMTF++ efficiency with and without the (i)RPC information added to the algorithm for the case of a single muon sample generated with and without PU information. The contribution of iRPC starts for  $|\eta| > 1.8$ , so that significant dips in efficiencies are seen around 2 and 2.2 for the case without the (i)RPC subsystem. The drops in both efficiencies for the regions of the Endcaps below the  $|\eta| = 1.8$  threshold reflect the expected behaviour of the algorithm due to detector geometry and resolution effects [2].

## Conclusion

The CMS Phase-2 upgrade of the Muon system and L1 Trigger system is designed to meet the requirements of HL-LHC. The upgrade includes new improved RPCs and better electronics across all subsystems, enhancing time resolution and increasing coverage in high-rapidity regions where particle density and PU are greatest. A major improvement is the upgrade to the Endcap Muon Track Finder, EMTF++, which now uses a DNN for track parameter assignment, providing better precision and reliability, compared to the previous boosted decision trees. Efficiency studies reveal that EMTF++ maintains high stability across  $p_T$  thresholds and benefits significantly from (i)RPC

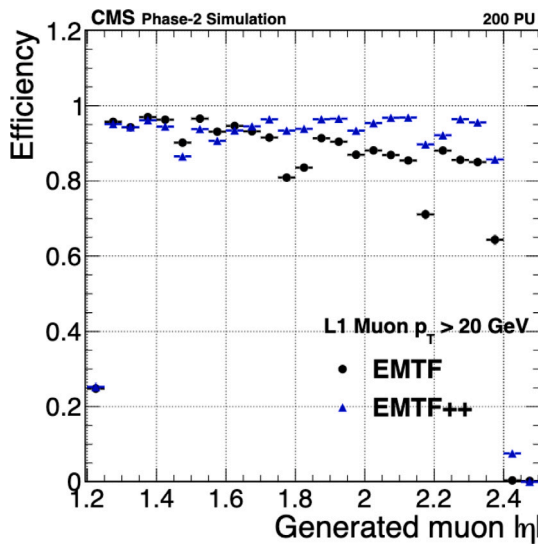


Fig. 3. Efficiencies for Endcap single muon samples with 200 average pileup events as a function of  $\eta$ , for muons with  $p_T > 20$  GeV and a  $L1p_T > 20$  GeV.

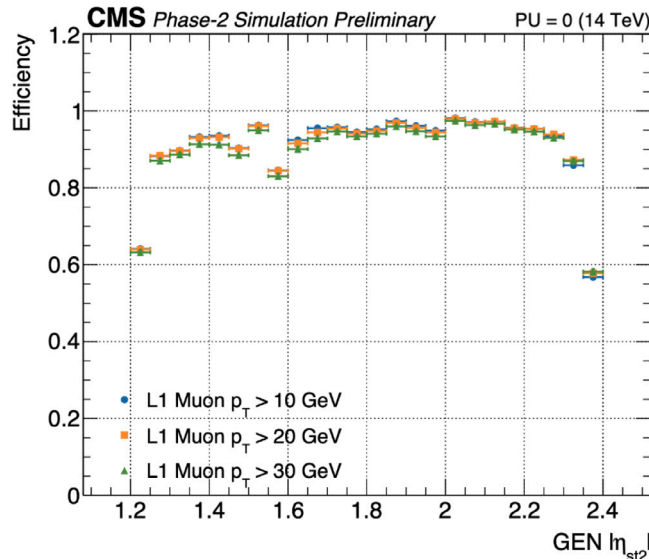


Fig. 4. Efficiencies of the algorithm for the sample containing (i)RPC information - the performance is stable when going to higher  $p_T$  cuts.

data, especially in the  $|\eta| > 1.8$  range, under high PU conditions. Without (i)RPC data, efficiency in this region drops, highlighting the critical role of these subsystems in achieving uniform performance. To enhance the model, timing information from (i)RPC subsystem will be included as input to the NN. Once trained, efficiency studies will be conducted with various  $p_T$  cuts and PU configurations to assess performance changes. Additionally, these analyses will be extended to different physics models, such as long-lived particles (LLP) decaying to muons, to evaluate the network's adaptability and efficiency across diverse scenarios.

#### Declaration of competing interest

The authors declare that they have no known competing financial interests or personal relationships that could have appeared to influence the work reported in this paper.

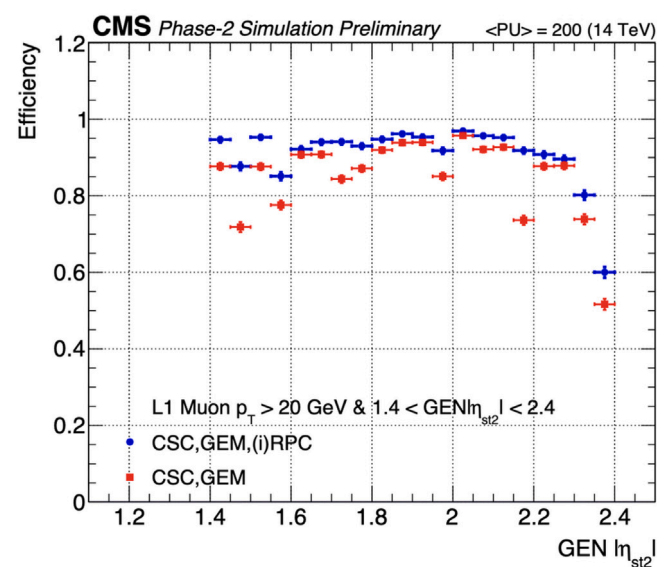
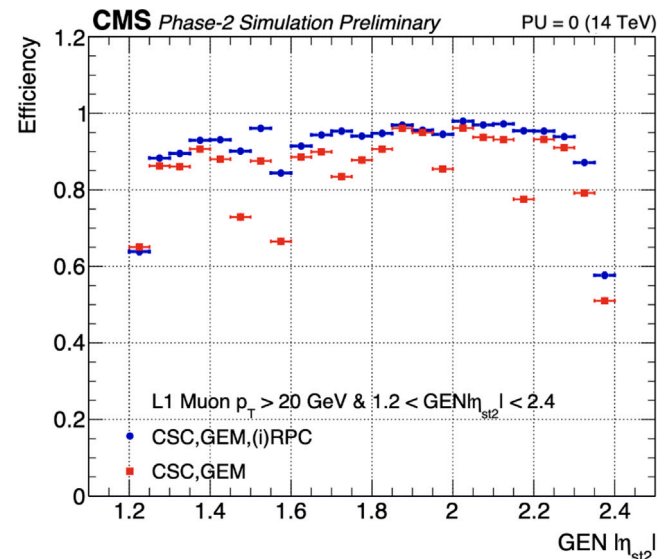


Fig. 5. Plots showing the different values of the EMTF++ efficiency with (blue circle) and without (red square) the (i)RPC information added to the algorithm for the case of a single muon final state sample (100k events) generated in the absence of PU (top) or with an average value of the PU of 200 (bottom). The algorithm was not optimized to account for the absence of the individual subsystems.

#### Acknowledgements

We would like to acknowledge the enduring support for the Upgrade of the CMS detector and the supporting computing infrastructure provided by the following funding agencies: FWO (Belgium); CNPq, CAPES and FAPERJ (Brazil); MES and BNSF (Bulgaria); CERN; CAS, MoST, and NSFC (China); MINCIENCIAS (Colombia); CEA and CNRS/IN2P3 (France); SRNSFG (Georgia); IPM (Iran); INFN (Italy); MSIP and NRF (Republic of Korea); BUAP, CINVESTAV, CONACYT, LNS, SEP, and UASLP-FAI (Mexico); PAEC (Pakistan); DOE and NSF (USA).

#### References

- [1] CMS Collaboration, in: The C.M.S. Collaboration (Ed.), The Phase-2 Upgrade of the CMS Muon Detectors, Tech. rep., CERN, Geneva, 2017, URL <https://cds.cern.ch/record/2283189>.
- [2] The C.M.S. Collaboration, CMS Collaboration, The Phase-2 Upgrade of the CMS Level-1 Trigger, Tech. rep., CERN, Geneva, 2020, URL <https://cds.cern.ch/record/2714892>.